Electronic Supplementary Material (ESI) for Journal of Materials Chemistry A.

Electronic Supplementary Information

Novel cobalt-doped molybdenum oxynitride quantum dots@N-doped carbon nanosheets with abundant oxygen vacancies for long-life rechargeable zinc-air batteries

Thanh Tuan Nguyen,[ab] Jayaraman Balamurugan,[a] Kin-Tak Lau,[b] Nam Hoon Kim,*[a] Joong Hee Lee*[ac]

[a]Advanced Materials Institute of Nano Convergence Technology (BK21 Four) & Dept. of Nano Convergence Technology, Jeonbuk National University, Jeonju, Jeonbuk, 54896, Republic of Korea.
[b]Faculty of Science, Engineering and Technology, Swinburne University of Technology, John St., Hawthorn, Melbourne, VIC, 3122, Australia.
[c]Carbon Composite Research Centre, Department of Polymer - Nano Science and Technology, Jeonbuk National University, Jeonju, Jeonbuk, 54896, Republic of Korea.

E-mail: nhk@jbnu.ac.kr; jhl@jbnu.ac.kr

1. Calculations

The RDE and RRDE measurements were carried out at different rotational speeds from 400 to 2800 rpm (400 rpm for each step) in an O_2-saturated 0.1 M KOH electrolyte. The number of electrons transferred in ORR was calculated from the Koutecky-Levich formula:[1]

$$\frac{1}{j_L} = \frac{1}{j_K} + \left(\frac{1}{0.62nFCD^{2/3}\upsilon^{-1/6}}\right)\omega^{-1/2} \tag{1}$$

where j_K is kinetic current density, n is the number of electron transfer, F is the Faraday constant (96,485 C mol^{-1}), C is the concentration of oxygen in the electrolyte (1.2×10^{-6} mol cm^{-3}), D is the diffusion coefficient of oxygen in the solution (1.9×10^{-5} cm^2 s^{-1}), υ is the dynamic viscosity of the aqueous 0.1 M KOH electrolyte (0.01 cm^2 s^{-1}), and ω is rotational speed.

The RRDE measurement was exemplified to investigate the 4 e$^-$ sensitivity. The H_2O_2 yield and electron transfer (n) were calculated by the following equations:[1]

$$n = \frac{4j_D}{j_D + \frac{j_R}{N}} \tag{2}$$

$$H_2O_2\ yield\ (\%) = \frac{\frac{2j_R}{N}}{j_D + \frac{j_R}{N}} \times 100 \tag{3}$$

where j_D and j_R is the Faradaic current on the disk and ring, respectively. N is the H_2O_2 collection coefficient of the ring (0.37).

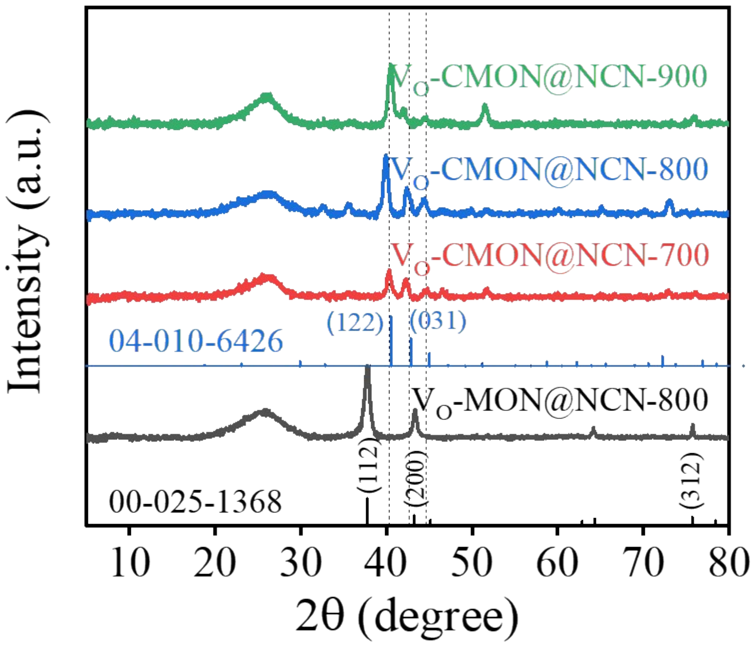

Fig. S1. The XRD patterns of V_O-CMON@NCN with different pyrolysis temperature

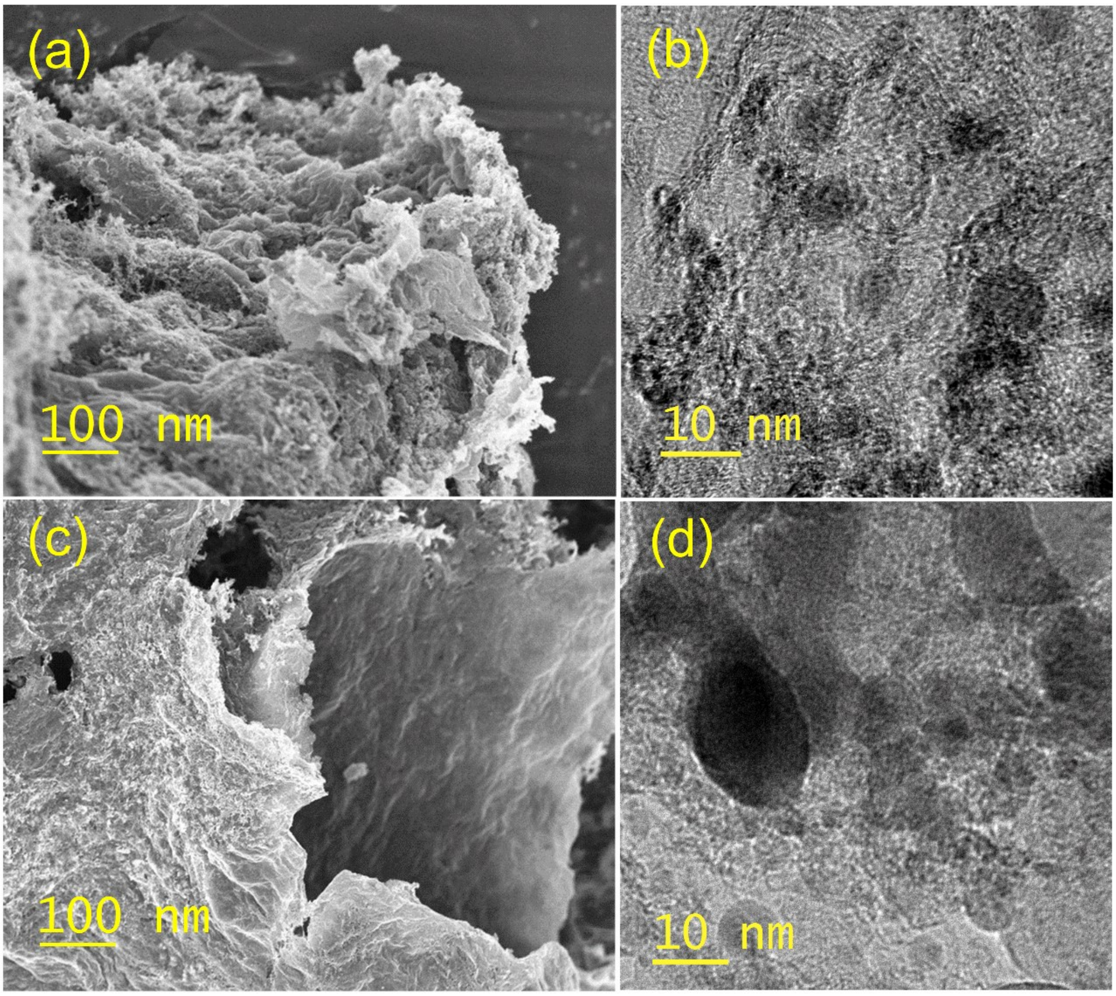

Fig. S2. SEM and HR-TEM images of (a, b) V_O-CMON@NCN-700 and (c, d) V_O-CMON@NCN-900.

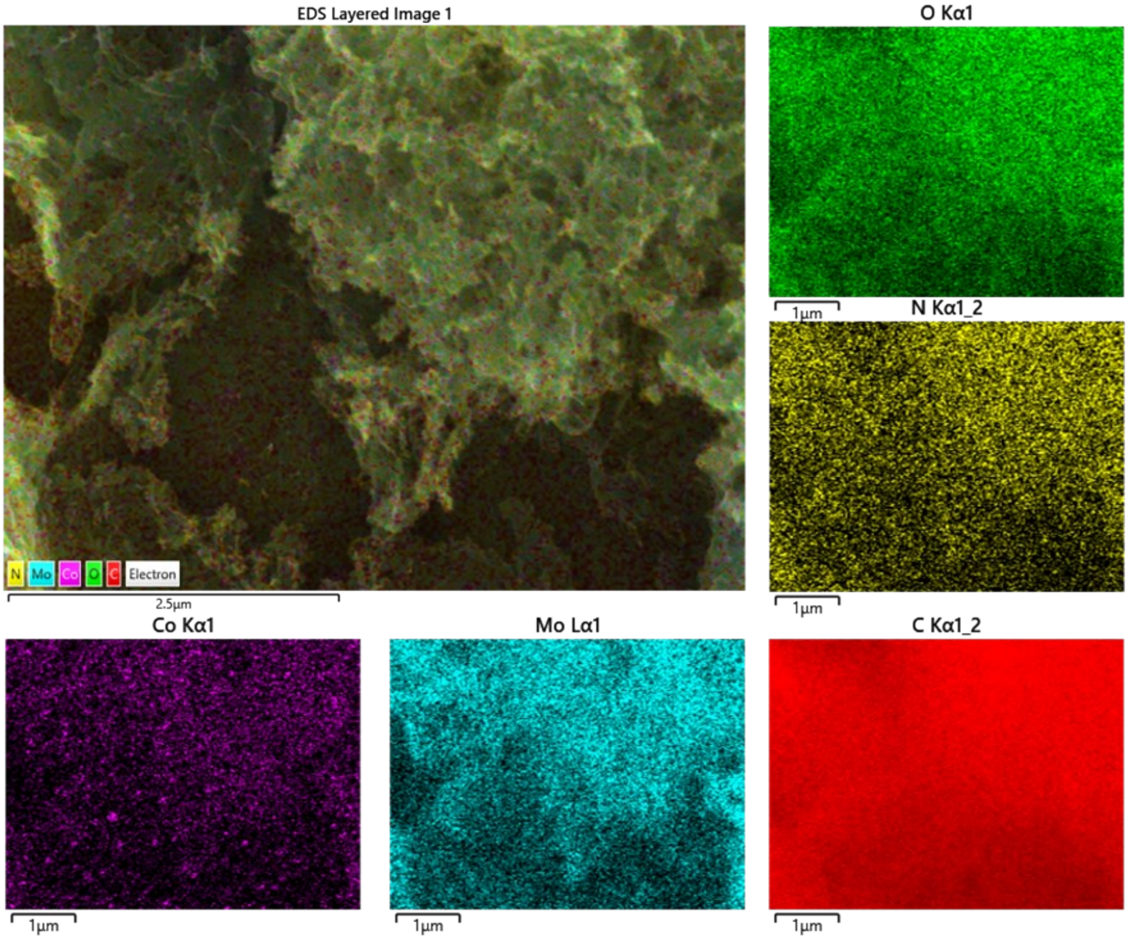

Fig. S3. SEM-EDS color mapping analysis of V_O-CMON-800@NCN and corresponding elemental distributions of Co, Mo, O, N, and C.

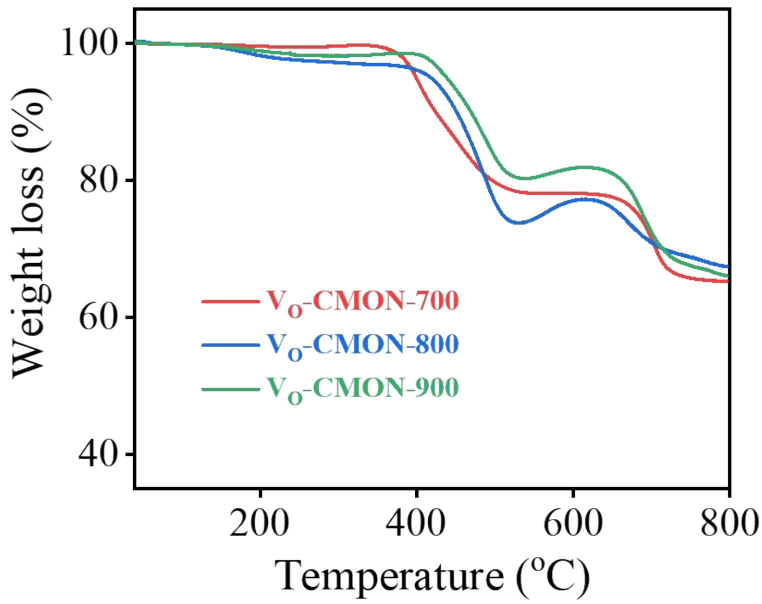

Fig. S4. The TGA of all materials with different pyrolysis temperature from 700 to 900 °C

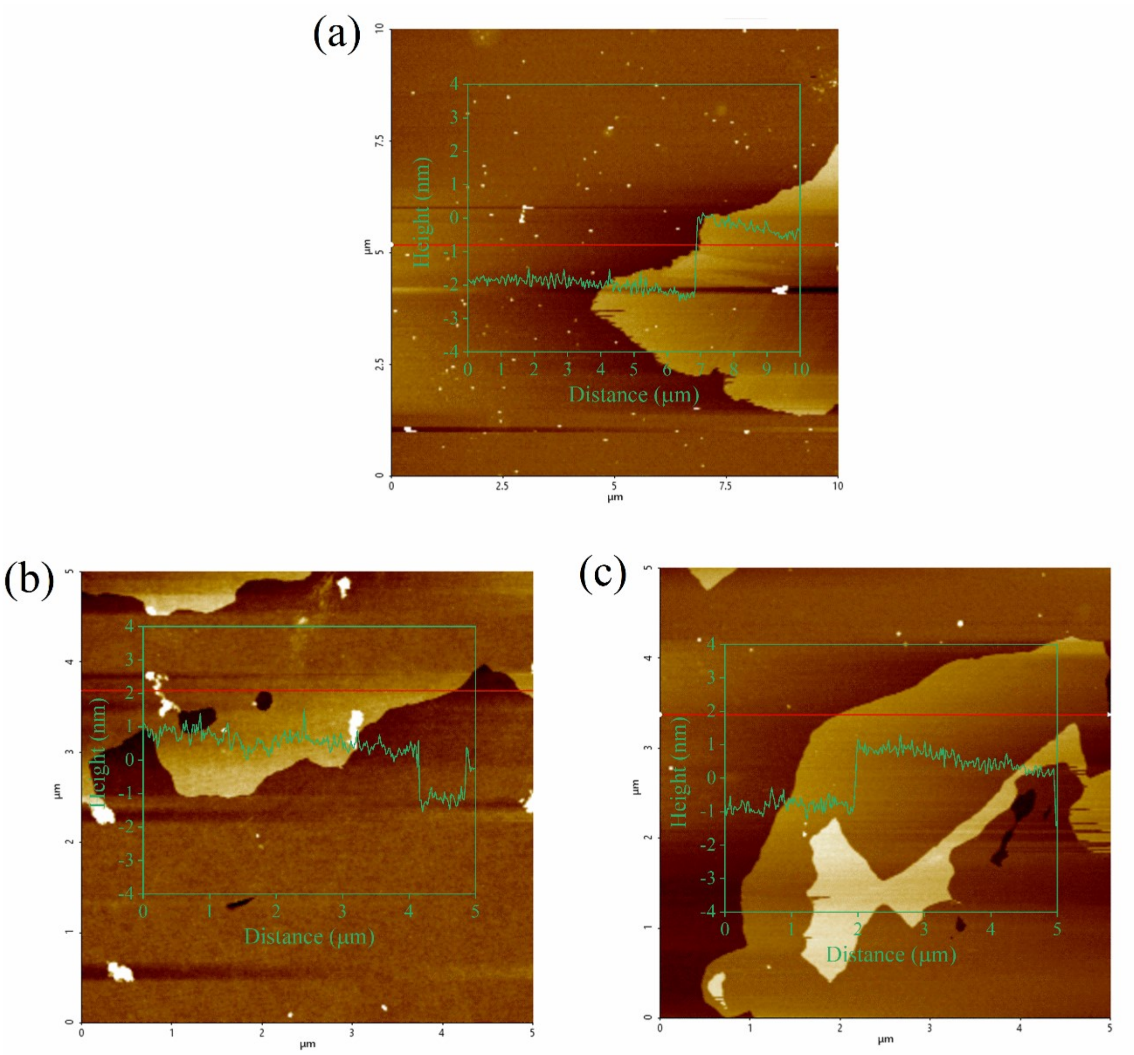

Fig. S5. AFM images for the (a) V_O-CMON@NCN-700; (b) V_O-CMON@NCN-800, and (c) V_O-CMON@NCN-900 nanohybrids.

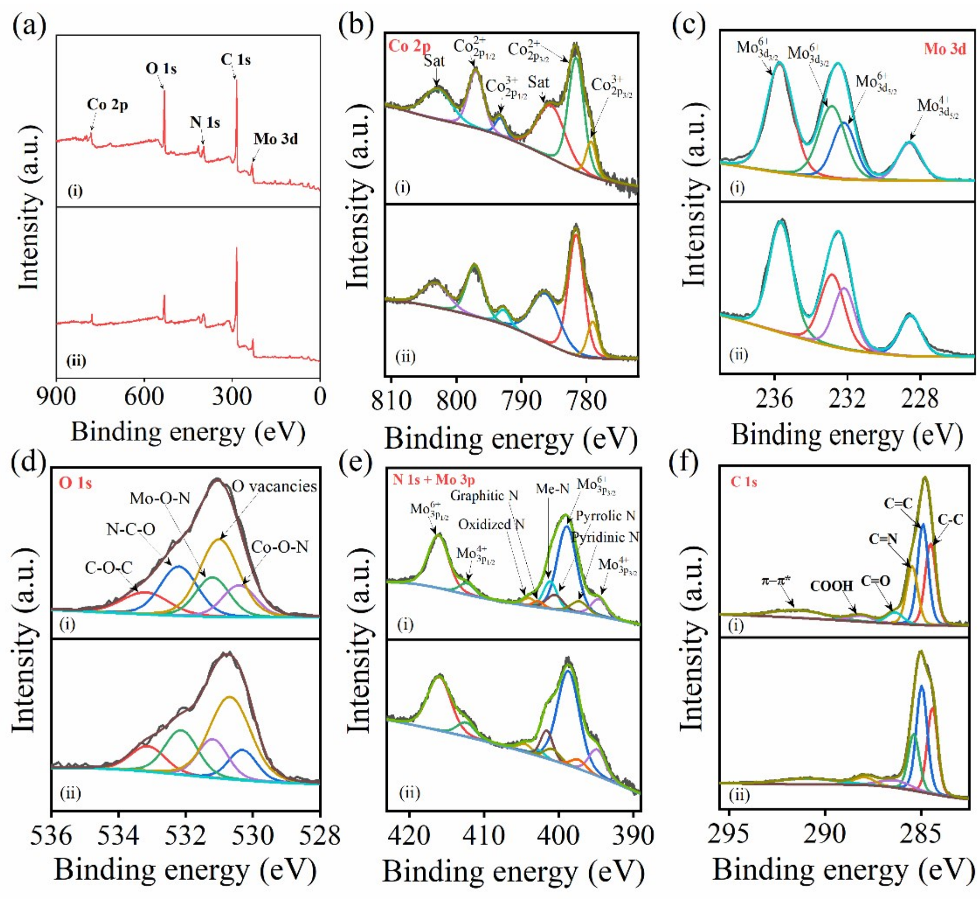

Fig. S6. (a) XPS survey and high-resolution XPS of (b) Co 2p, (c) Mo 3d, (d) O 1s, (e) N 1s + Mo 3p, (f) C 1s for (i) V_O-CMON@NCN-700 and (ii) V_O-CMON@NCN-900 nanohybrids.

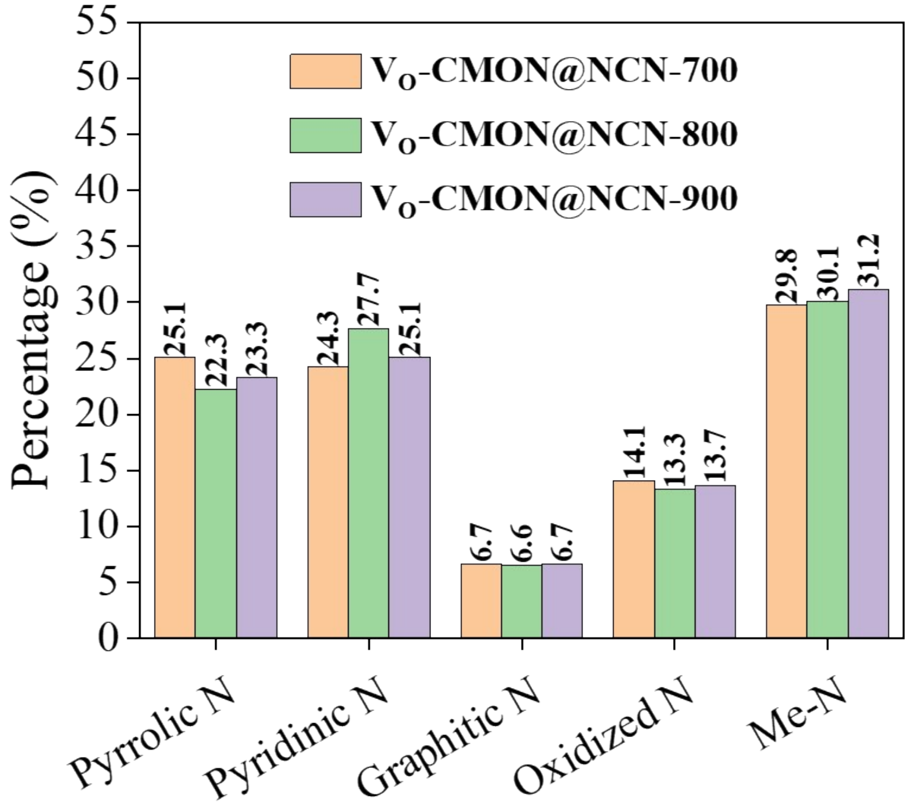

Fig. S7. The percentage of pyrrolic N, pyridinic N, graphitic N, oxidized N and Me-N in all catalyst materials.

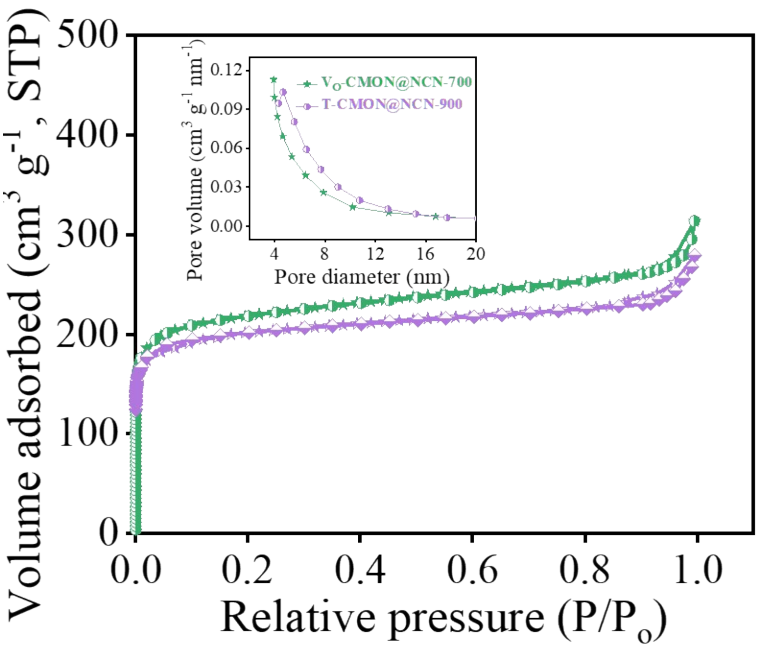

Fig. S8. BET of V_O-CMON@NCN-700; TGA V_O-CMON@NCN-900

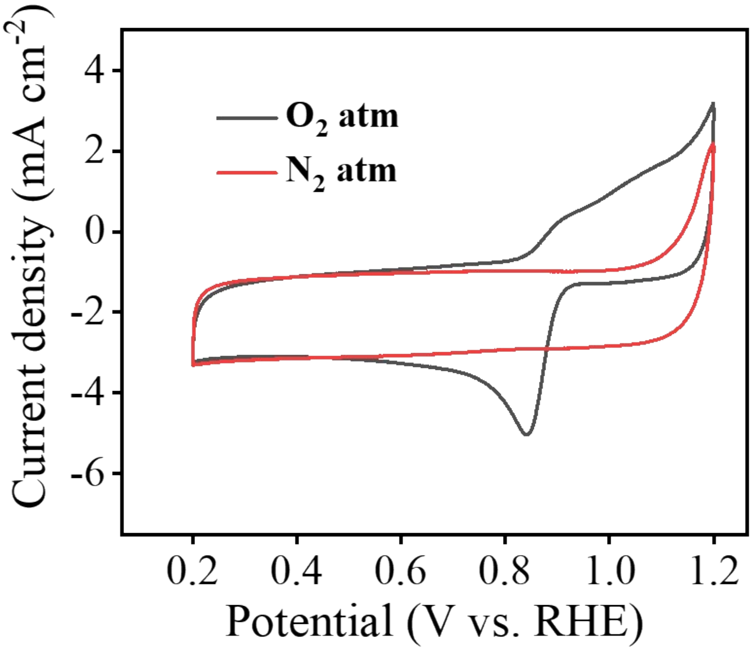

Fig. S9. The CV curves of V_O-CMON@NCN-800 at a fixed scan rate of 50 mV s^{-1} in N_2 and O_2-saturated 0.1 M KOH electrolyte.

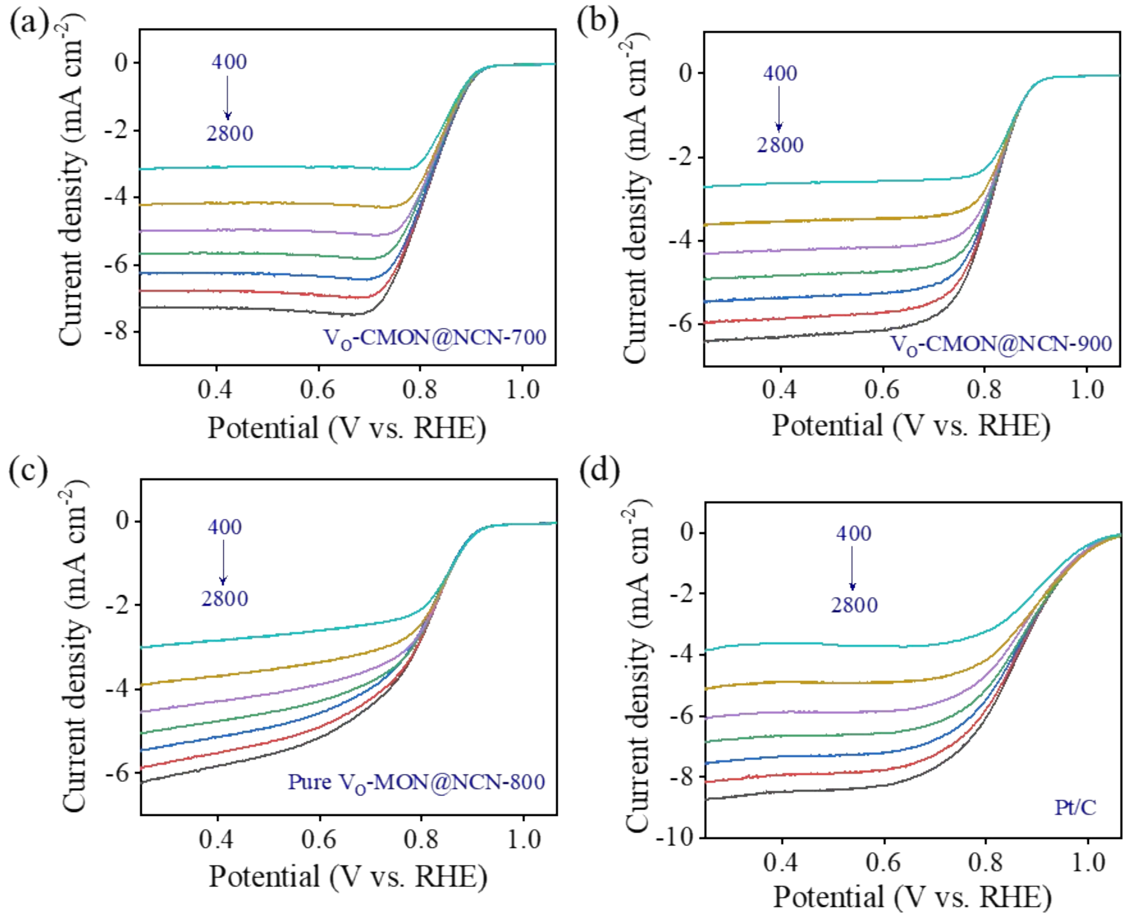

Fig. S10. LSV at different rotation speed from 400 to 2800 rpm of (a) V_O-CMON@NCN-700, (b) V_O-CMON@NCN-900, (c) Pure V_O-MON@NCN-800, and Pt/C.

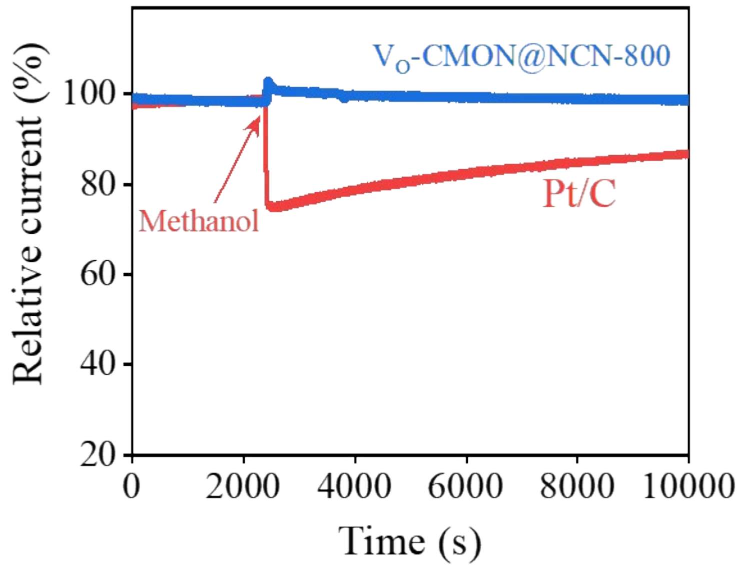

Fig. S11. Methanol-tolerance evaluation of V_O-CMON@NCN-800 and Pt/C in O_2-saturated 0.1 m KOH solution.

.

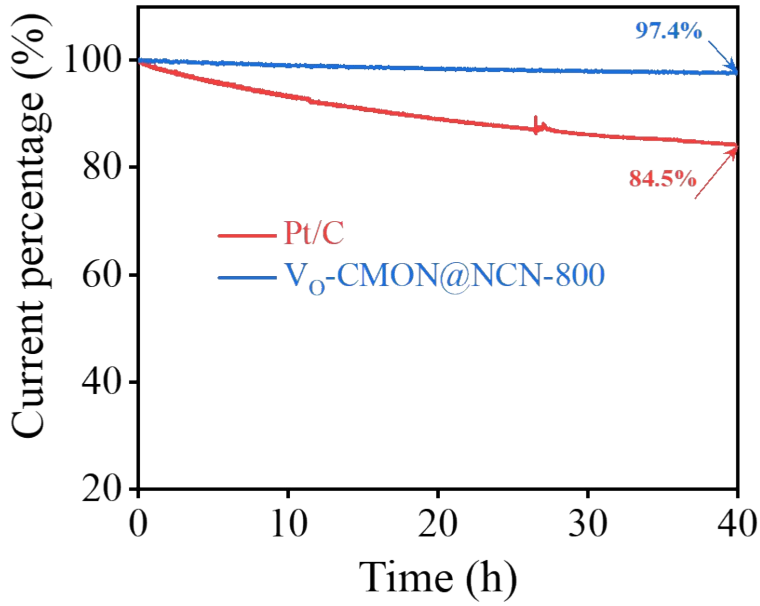

Fig. S12. Long-term stability of V_O-CMN@NCN-800 and Pt/C catalyst after 40 h.

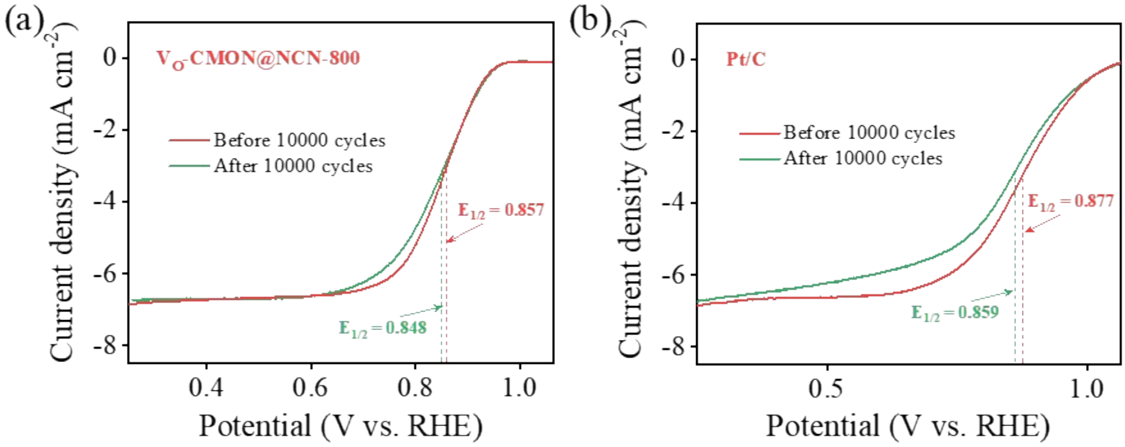

Fig. S13. LSV of V_O-CMON@NCN-800 and Pt/C at 1600 rpm before and after 10000 CV cycles

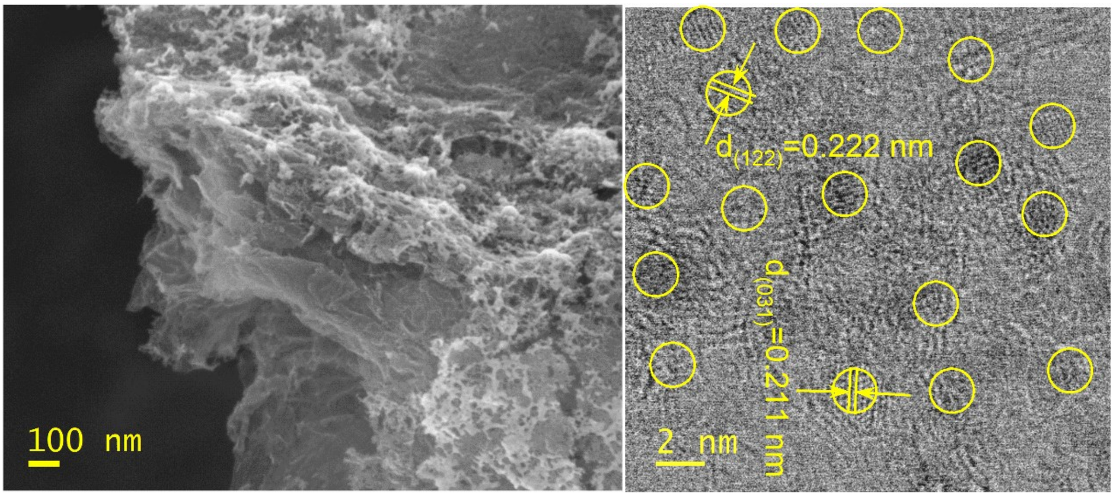

Fig. S14. SEM and TEM images of V_O-CMON@NCN-800 catalyst after 10000 CV cycles ORR stability test.

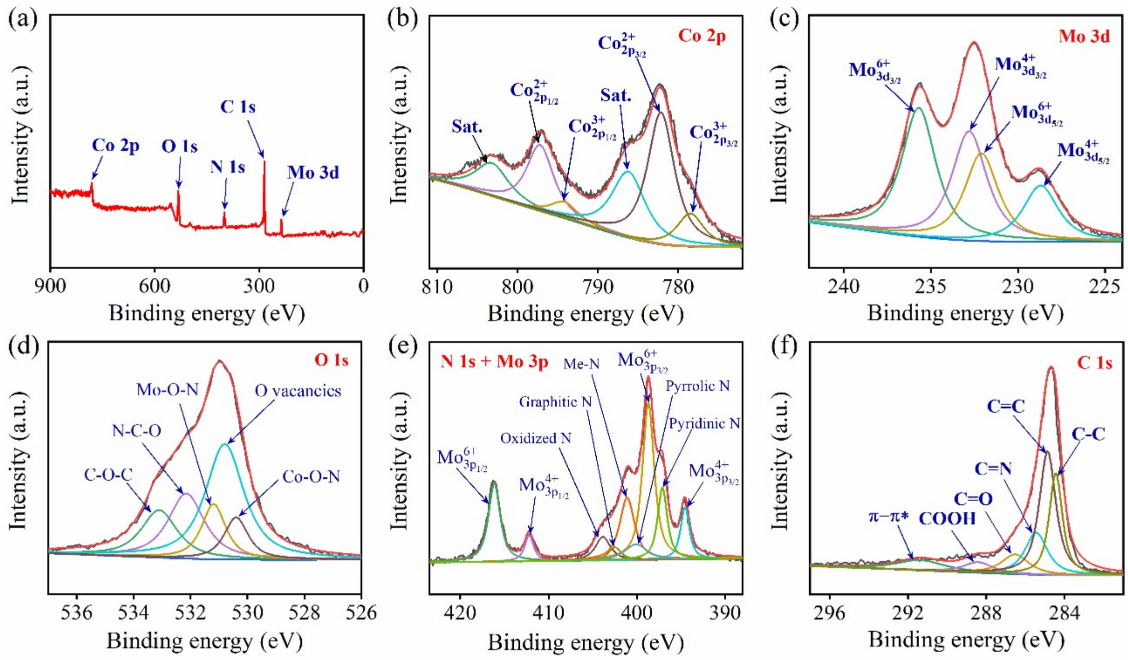

Fig. S15. XPS of V_O-CMON@NCN-800 catalyst after 10000 CV cycles ORR stability test.

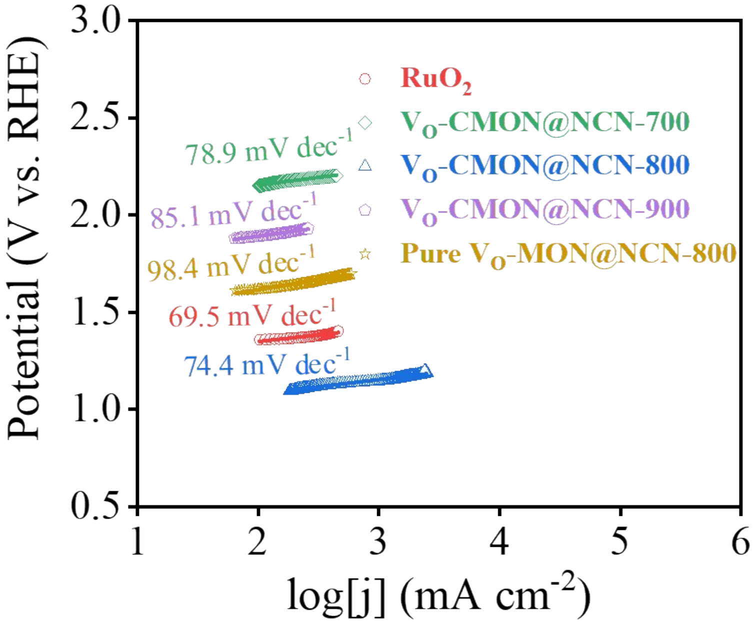

Fig. S16. Tafel plots of as-obtained catalysts toward OER measurement.

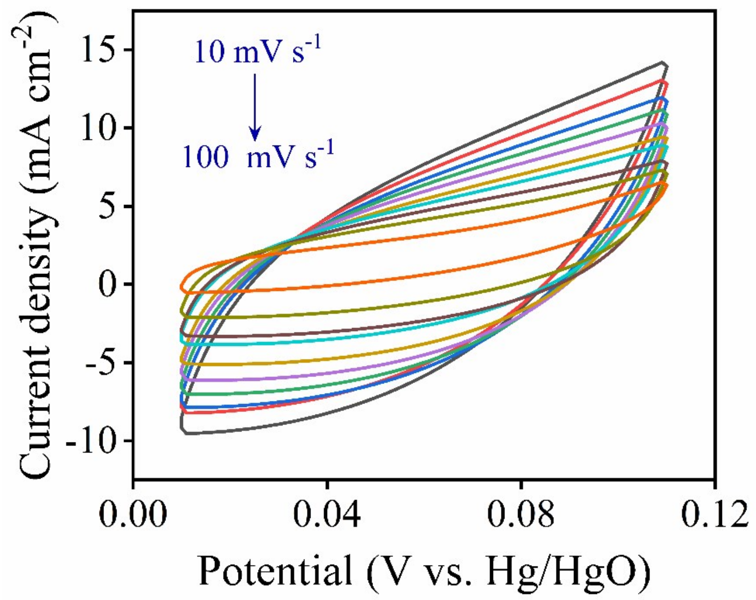

Fig. S17. CV curves of V_O-CMON@NCN-800 at different sweep rate of 10 to 100 mV s^{-1}.

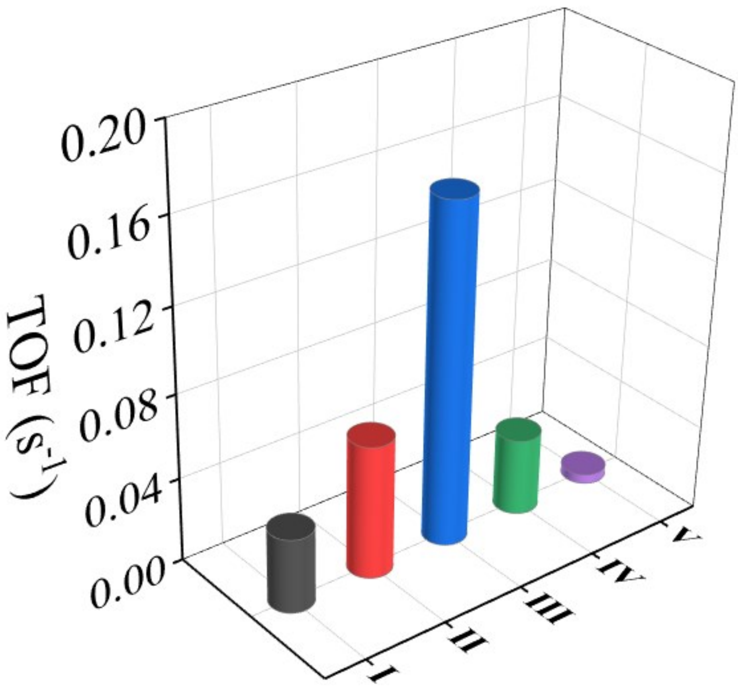

Fig. S18. TOF at the overpotential of 260 mV for the (I) RuO_2, (II) V_O-CMON@NCN-700, (III) V_O-CMON@NCN-800, (IV) V_O-CMON@NCN-900, and (V) V_O-MON@NCN-800 catalysts.

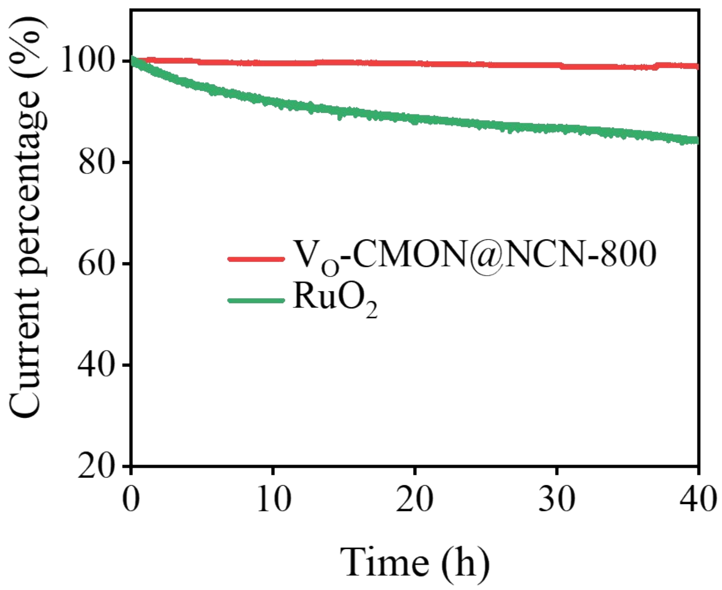

Fig. S19. Long-term stability of V_O-CMON@NCN-800 and RuO_2 catalyst after 40 h.

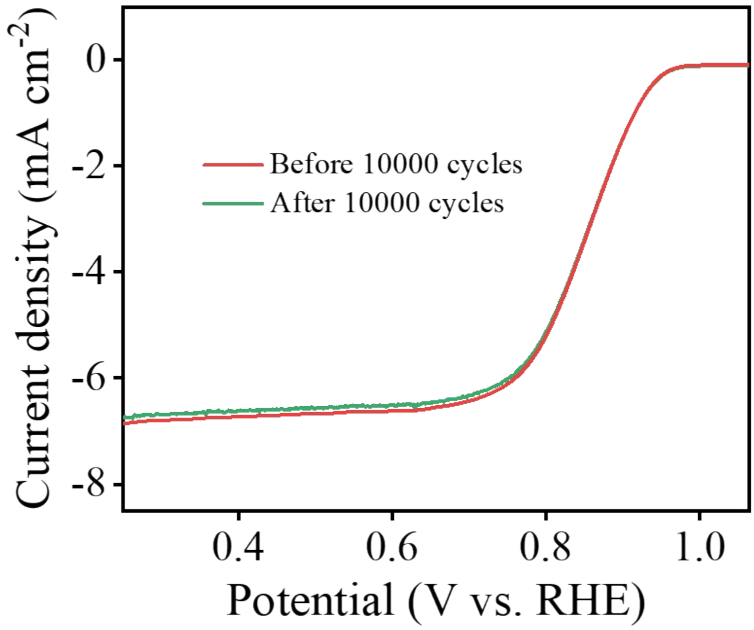

Fig. S20. LSV curves of V_O-CMON@NCN-800 before and after 10000 CV cycles.

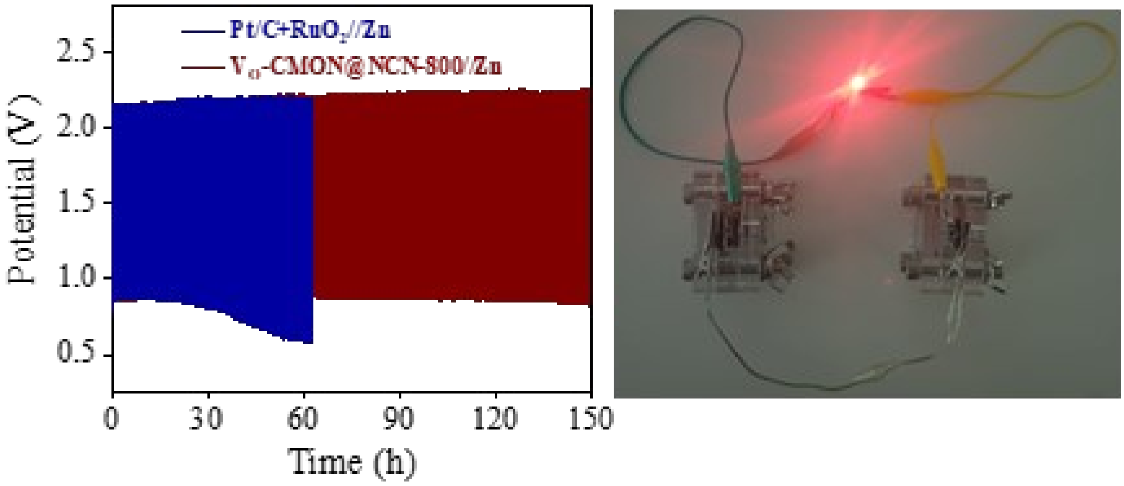

Fig. S21. Cycle stability of ZABs at a high current density of 20 mA cm^{-2} and a series-connected ZABs powered a red LED.

Table S1. Element composition of all catalyst materials estimated from ICP-AES

Samples	Co [wt%]	Mo [wt%]	N [wt%]	O [wt%]	C [wt%]
Pure V_O-MON@NCN		26.7	14.4	16.4	42.5
V_O-CMON@NCN-700	17.3	22.1	13.2	13.1	34.3
V_O-CMON@NCN-800	17.1	19.9	14.5	12.8	35.7
V_O-CMON@NCN-800	16.9	19.8	13.9	13.5	35.9

Co, Mo, O, N, and C contents were detected by ICP-AES measurement.

Table S2. The catalytic activities of the reported non-noble bifunctional catalysts for ORR.

ORR catalysts	Catalyst loading (mg cm^{-2})	Electrolyte	$E_{1/2}$ (V vs. RHE)	Ref#
V_O-CMON@NCN-800	0.1	0.1 M KOH	0.857	This work
Ni_3Fe/N-C sheets	0.13	0.1 M KOH	0.78	[2]
NiFe-LDH/Co,NCNF	0.79	0.1 M KOH	0.79	[3]
N-CG–CoO	0.1	0.1 M KOH	0.78	[4]
Mn oxide	-	0.1 M KOH	0.73	[5]
NiFe@NCX	0.40	0.1 M KOH	0.86	[6]
Co/Co_3O_4@PGS	0.3	0.1 M KOH	0.89	[7]
NiO/CoN PINWs	0.20	0.1 M KOH	0.68	[8]
S,N-Fe/N/C-CNT	0.25	0.1 M KOH	0.84	[9]
GH-BGQD	-	0.1 M KOH	0.73	[10]
Ni-MnO/rGO aerogel	0.25	0.1 M KOH	0.78	[11]
NiCo/PFC	0.13	0.1 M KOH	0.77	[12]
NC@Co-NGC	-	0.1 M KOH	0.82	[13]
Co-N_x-C	0.25	0.1 M KOH	0.80	[14]
CoZn-NC700	-	0.1 M KOH	0.84	[15]
$NiCo_3S_4$/N-CNT	0.25	0.1 M KOH	0.80	[16]

Table S3. The catalytic activities of the reported non-noble catalysts for OER.

OER catalysts	Catalyst loading (mg cm^{-2})	Electrolyte	$E_{j=10}$ (V vs. RHE)	Ref#
V_O-CMON@NCN-800	0.1	0.1 M KOH	1.47	This work
Ni_3Fe/N-C sheets	0.13	0.1 M KOH	1.60	2
NiFe-LDH/Co,NCNF	0.79	0.1 M KOH	1.54	3
N-CG–CoO	0.1	0.1 M KOH	1.37	4
Mn oxide	-	0.1 M KOH	1.77	5
NiFe@NCX	0.40	0.1 M KOH	1.55	6
Co/Co_3O_4@PGS	0.3	0.1 M KOH	1.58	7
NiO/CoN PINWs	0.20	0.1 M KOH	1.53	8
S,N-Fe/N/C-CNT	0.25	0.1 M KOH	1.60	9
GH-BGQD	-	0.1 M KOH	1.60	10
Ni-MnO/rGO aerogel	0.25	0.1 M KOH	1.60	11
NiCo/PFC	0.13	0.1 M KOH	1.62	12
NC@Co-NGC	-	0.1 M KOH	1.64	13
Co-N_x-C	0.25	0.1 M KOH	1.75	14
CoZn-NC700	-	0.1 M KOH	1.63	15
$NiCo_3S_4$/N-CNT	0.25	0.1 M KOH	1.60	16
NPMC-1000	-	0.1 M KOH	1.42	17

Table S4. The comparative performance of the ZAB with recently reported non-noble air cathode based ZAB devices in alkaline electrolytes.

Air cathode	OCP (V)	Power density (mW cm^{-2})	Specific capacity (mAh g_{zn}^{-1}@mA cm^{-2})	Energy density (W h g^{-1} @mA cm^{-2})	Durability (h)	Ref#
V_O-CMON@NCN-800	1.403	143.7	-	841	500 h	This work
Co_4N/CNW/CC	1.40	174	-	-	1200s/cycle for 408 cycles; 136 h	18
NPMC-1100	1.48	55	735@5	835@5	600 cycles/100 h	17
NiFe@NC_X	-	87	583.7@10	732.3@10	600s/200 cycles; 33.33 h	6
NiO/CoN PINWs	1.46	79.6	690@5	945@5	600 s/cycle for 25 cycles; 8.3 h	8
GH-BGQD	1.48	112	-	810	70 h	10
Ni-MnO/rGO aerogel	-	123	758@5	930@5	100 cycles	11
CoZn-NC-700	1.42	152	578@10	694@10	600 s/cycle for 385 cycles	15
NGM-Co	1.44	152	749.4@20	840@20	1350s/cycle for 160 cycles; 60 h	14
C-MOF-C_2-900	1.46	105	741@10	-	300 cycles; 120 h	19
CoS_x@PCN/rGO	1.38	-	-	634	400s /cycle for 394 cycle; 43.8 h	20
N-GCNT/FeCo	1.48	89.3	872.2@100	653.2@100	-	21
$ZnCo_2O_4$/N-CNT	1.47	82.3	428.47@10	595.57@10	600s/ cycle for 23 cycles; 320 min	22
$Fe_{0.5}Co_{0.5}O_x$	1.44	86	709@25	806@25	120 h	23
$Co_3FeS_{1.5}(OH)_6$		113.1	898@20	-	108 cycles; 36 h	24
N-GRW	1.46	65	873@20		150 cycles/160 h	25
Meso-CoNC@GF	1.51	154.4	-	-	630 cycles; 105 h	26
CuS/NiS_2	1.44	172.4	775@5	1015.2@5	200 cycles; 83 h	27

References

1. Z. Yang, C. Zhao, Y. Qu, H. Zhou, F. Zhou, J. Wang, Y. Wu and Y. Li, *Adv. Mater.*, 2019, **31**, 1808043.
2. G. Fu, Z. Cui, Y. Chen, Y. Li, Y. Tang and J. B. Goodenough, *Adv. Energy Mater.*, 2017, **7**, 1601172.
3. Q. Wang, L. Shang, R. Shi, X. Zhang, Y. Zhao, G. I. N. Waterhouse, L.-Z. Wu, C.-H. Tung and T. Zhang, *Adv. Energy Mater.*, 2017, **7**, 1700467.
4. S. Mao, Z. Wen, T. Huang, Y. Hou and J. Chen, *Energy Environ. Sci.*, 2014, **7**, 609-616.
5. Y. Gorlin and T. F. Jaramillo, *J. Am. Chem. Soc.*, 2010, **132**, 13612-13614.
6. J. Zhu, M. Xiao, Y. Zhang, Z. Jin, Z. Peng, C. Liu, S. Chen, J. Ge and W. Xing, *ACS Catal.*, 2016, **6**, 6335-6342.
7. Y. Jiang, Y.-P. Deng, J. Fu, D. U. Lee, R. Liang, Z. P. Cano, Y. Liu, Z. Bai, S. Hwang, L. Yang, D. Su, W. Chu and Z. Chen, *Adv. Energy Mater.*, 2018, **8**, 1702900.
8. J. Yin, Y. Li, F. Lv, Q. Fan, Y.-Q. Zhao, Q. Zhang, W. Wang, F. Cheng, P. Xi and S. Guo, *ACS Nano*, 2017, **11**, 2275-2283.
9. P. Chen, T. Zhou, L. Xing, K. Xu, Y. Tong, H. Xie, L. Zhang, W. Yan, W. Chu, C. Wu and Y. Xie, *Angew. Chem., Int. Ed.*, 2017, **56**, 610-614.
10. T. V. Tam, S. G. Kang, M. H. Kim, S. G. Lee, S. H. Hur, J. S. Chung and W. M. Choi, *Adv. Energy Mater.*, 2019, **9**, 1900945.
11. G. Fu, X. Yan, Y. Chen, L. Xu, D. Sun, J.-M. Lee and Y. Tang, *Adv. Mater.*, 2018, **30**, 1704609.
12. G. Fu, Y. Chen, Z. Cui, Y. Li, W. Zhou, S. Xin, Y. Tang and J. B. Goodenough, *Nano Lett.*, 2016, **16**, 6516-6522.
13. S. Liu, Z. Wang, S. Zhou, F. Yu, M. Yu, C.-Y. Chiang, W. Zhou, J. Zhao and J. Qiu, *Adv. Mater.*, 2017, **29**, 1700874.
14. C. Tang, B. Wang, H.-F. Wang and Q. Zhang, *Adv. Mater.*, 2017, **29**, 1703185.
15. B. Chen, X. He, F. Yin, H. Wang, D.-J. Liu, R. Shi, J. Chen and H. Yin, *Adv. Funct. Mater*, 2017, **27**, 1700795.
16. X. Han, X. Wu, C. Zhong, Y. Deng, N. Zhao and W. Hu, *Nano Energy*, 2017, **31**, 541-550.
17. J. Zhang, Z. Zhao, Z. Xia and L. Dai, *Nat. Nanotechnol.*, 2015, **10**, 444-452.
18. F. Meng, H. Zhong, D. Bao, J. Yan and X. Zhang, *J. Am. Chem. Soc.*, 2016, **138**, 10226-10231.
19. M. Zhang, Q. Dai, H. Zheng, M. Chen and L. Dai, *Adv. Mater.*, 2018, **30**, 1705431.
20. W. Niu, Z. Li, K. Marcus, L. Zhou, Y. Li, R. Ye, K. Liang and Y. Yang, *Adv. Energy Mater.*, 2018, **8**, 1701642.
21. C.-Y. Su, H. Cheng, W. Li, Z.-Q. Liu, N. Li, Z. Hou, F.-Q. Bai, H.-X. Zhang and T.-Y. Ma, *Adv. Energy Mater.*, 2017, **7**, 1602420.
22. Z. Q. Liu, H. Cheng, N. Li, T. Y. Ma and Y. Z. Su, *Adv. Mater.*, 2016, **28**, 3777-3784.
23. L. Wei, H. E. Karahan, S. Zhai, H. Liu, X. Chen, Z. Zhou, Y. Lei, Z. Liu and Y. Chen, *Adv. Mater.*, 2017, **29**, 1701410.
24. H.-F. Wang, C. Tang, B. Wang, B.-Q. Li and Q. Zhang, *Adv. Mater.*, 2017, **29**, 1702327.
25. H. B. Yang, J. Miao, S.-F. Hung, J. Chen, H. B. Tao, X. Wang, L. Zhang, R. Chen, J. Gao, H. M. Chen, L. Dai and B. Liu, *Sci. Adv.*, 2016, **2**, e1501122.
26. S. Liu, M. Wang, X. Sun, N. Xu, J. Liu, Y. Wang, T. Qian and C. Yan, *Adv. Mater.*, 2018, **30**, 1704898.
27. L. An, Y. Li, M. Luo, J. Yin, Y.-Q. Zhao, C. Xu, F. Cheng, Y. Yang, P. Xi and S. Guo, *Adv. Funct. Mater*, 2017, **27**, 1703779.